9 Thoracoabdominal Approach for Tumors of the Thoracolumbar Spine

A. Karim Ahmed, Daniel M. Sciubba, and Feng Wei

Anatomic and Biomechanical Considerations

The thoracolumbar region (T11–L2) serves as an anatomic transition zone between the thorax and abdomen, a structural transition zone between the kyphotic thoracic and lordotic lumbar spine, and a dynamic transition zone between the semi-rigid thoracic and mobile lumbar spine.

The thoracolumbar spine, from T11 to L2, has unique structural and biomechanical challenges. Held in place by the ribs, the semirigid thoracic spine does not significantly contribute to mobility. This is in contrast to caudal lumbar segments which impart the majority of torso flexion and extension, particularly from L2 to L4.

Twelve paired ribs correspond to 12 thoracic vertebrae, containing superior and inferior costal facets for the articulation of the rib head, and an articular facet joint for articulation with the tubercle of the rib. The first seven paired ribs comprise the "true ribs," and the subsequent five comprise the "false ribs"—the latter two of which are known as "floating ribs" and lack costal articulation with the sternum.

A. Karim Ahmed · D. M. Sciubba
Department of Neurosurgery, The Johns Hopkins Hospital, Baltimore, MD, USA

F. Wei (✉)
Peking University Third Hospital, Department of Orthopedics, Beijing, China
e-mail: weifeng@bjmu.edu.cn

With the exception of the T1 nerve root, responsible for finger abduction, the majority of thoracic motor nerves do not innervate critical muscles required for mobility or function, unlike in the cervical and lumbar spine. The anterior rami from T1 to T11 provide the intercostal nerves, which travel along the caudal aspect of the rib in the neurovascular bundle, located in between the internal intercostal muscle and innermost intercostal muscle, innervating skin and muscle of the chest and abdomen. Dermatomal innervation of the areola, umbilicus, and lower abdominal wall correspond to nerve roots from T4, T10, and T12 (subcostal), respectively. Hip flexion is mostly performed by the iliopsoas muscle, supplied in large part by the L2 nerve root. The upper lumbar segments from L1 to L3 innervate the psoas major muscle, via the lumbar plexus. Iliacus is innervated by the femoral nerve from L2 to L4.

The costal pleura, bordering the inner surface of the ribs, and parietal pleura represent the superficial boundary of the pleural space—bordered deeply by the visceral pleura. The diaphragmatic portion of the parietal pleura overlies the diaphragm, innervated by the phrenic nerve (C3–C5) and crucial for breathing function. Separating the thorax from the abdomen, the diaphragm is a sheet of muscle with two main components: the peripheral muscle and the central tendon. Including the opening for the inferior vena cava (~T8), the central tendon aponeurosis is an insertion point for respiratory muscles and essential to reduce pressure in the pleural space

D. M. Sciubba (ed.), *Spinal Tumor Surgery*, https://doi.org/10.1007/978-3-319-98422-3_9

during inspiration. The peripheral muscles may be subdivided into the sternal, costal, and lumbar portions. The esophageal and aortic hiatus are formed by the peripheral muscle, at ~T10 and ~T12, respectively. The aortic hiatus allows for the passage of the aorta, azygos vein, hemiazygos vein, and thoracic duct. The psoas and quadratus lumborum muscles form the posterolateral border of the diaphragm, abutting the median and lateral arcuate ligaments. The paired tendinous crus of the diaphragm are tethered to the anterior longitudinal ligament of the lumbar vertebrae: the right (longer) crus attaches from L1 to L3 and the left attaches from L1 to L2 [1–7].

Operative Technique

Choosing Surgical Approach

The location of pathology and required exposure are critical to determine the best surgical approach. Anterior access to the thoracic spine, from T5 to T10, may be accomplished with a thoracotomy. For lesions of T5 or T6, the similarly numbered rib is removed (n). At T7 and T8, however, the rib of the suprajacent level is removed (n − 1). Removal of the rib two levels cranial to the lesion is required for exposure of T9 and T10 (n − 2). In the upper lumbar spine, however, anterior access may be performed via a retroperitoneal approach. As such, the thoracoabdominal approach is a combined thoracotomy and retroperitoneal exposure, with possible diaphragmatic detachment, for ventral access of the thoracolumbar junction, when either approach is not sufficient alone. The thoracoabdominal approach may be supplemented with a staged posterior approach for larger primary neoplasms requiring en bloc resection [8–11].

Patient Positioning

The patient is placed in the left lateral decubitus position. A left-sided thoracolumbar approach is favored due to large size and limited mobility of the liver on the right, compared with the contralateral spleen. Vascular injury to the left-sided thick-walled aorta is also considered to be easier to repair, compared to the right-sided vena cava; the former may be easier to mobilize, especially in the setting of radiation-induced retroperitoneal fibrosis [9].

Thoracoabdominal Exposure

An oblique flank skin incision is made from the 10th rib to the abdominal wall. Posterior retraction of the latissimus dorsi may be performed during muscle dissection. The rib is identified and subperiosteally dissected from its subcutaneous and muscular attachments (i.e., serratus anterior, latissimus dorsi, and intercostal muscles) on its superior border, thereby avoiding the neurovascular bundle. The rib may be resected for improved operative exposure, and the healthy bone is utilized for bone grafting. The rib is followed around to the costal margin, with careful dissection of the external and internal oblique muscles. Excessive dissection can result in abdominal flank bulging, pain, and weakness [8]. Division of the transversalis fascia, deep into the costal margin, exposes the peritoneum.

The peritoneum is dissected free from the bordering psoas, quadratus lumborum, and diaphragm to enter the retroperitoneal space. Ventral retraction of the peritoneum, posterior reflection of the psoas muscle, and detachment of the posterolateral diaphragm aid in exposure to the anterior spinal column. The diaphragm may be entered at its attachments with the median/lateral arcuate ligaments or crus. One must be mindful to preserve the distal muscular component of the diaphragm for repair and the central portion containing the phrenic nerve.

Detachment of the diaphragm, with gentle cranial retraction of the lung, exposes the diaphragmatic portion of the parietal pleura. Access to the lower thoracic spine and thoracolumbar junction may be accomplished by sharply incising the parietal pleura. Dissection of the segmental vessels allows for exposure of the anterior disk spaces and vertebral bodies but should be carefully performed due to the risk of hemorrhage. A preoperative angiogram of the artery of Adamkiewicz may be warranted if a large amount of lower thoracic

segmental vessels will be sacrificed. In order to preserve collateral circulation nerve and/or spinal cord (i.e., radicular artery, anterior spinal artery), ligation of the segmental vessels should occur at the anterior vertebral body. Retroperitoneal lymphatics (i.e., thoracic duct, cisterna chyli) should also be approached with caution in order to avoid the development of postoperative lymphoceles. Bipolar electrocautery, cottonoids, and hemostatic agents are useful to maintain hemostasis throughout the case [9–11].

Decompression

With the anterior spinal column exposed, the annulus of the intervertebral disk spaces may be sharply incised in preparation for discectomy. During this process, the great vessels should be mobilized anteriorly to prevent vascular injury. A high-speed burr, Leksell rongeurs, and Kerrison punch are useful to remove the disks above and below the diseased level. Disk fragments are taken piecemeal with pituitary rongeurs, and the posterior longitudinal ligament is removed with a Kerrison punch. Corpectomy is performed by first removing the rib head and proximal pedicle. Removal of the proximal pedicle exposes the dura [9–11].

Reconstruction and Instrumentation

Anterior column support is accomplished with the placement of an expandable cage in the vertebral defect and may be packed with healthy autologous (i.e., resected rib) bone, or allograft. A lateral screw-rod system, or plate, stabilizes the segment above and below. Posterior transpedicular screw and rod instrumentation may be appropriate to obtain added stability following extensive resection [9–11].

Closure

Closure is initiated in a watertight fashion. If the diaphragm was taken down during the exposure, a large-bore chest tube is placed, and primary repair of the diaphragm is performed with non-absorbable sutures. The parietal pleura may be sutured, and rib-approximating sutures close the thoracic cavity. The intercostal muscles, abdominal wall, serratus anterior, and latissimus dorsi muscles are closed, in a layered fashion, with nonabsorbable sutures. The fascia is reapproximated with 0 Vicryl, with reapproximation of the subcutaneous layer. The subcuticular layer may be closed with 3–0 Vicryl sutures [9, 10].

Case Presentation

This 63-year-old female presented with a 3-year history of an enlarging mass in the left side of her back, accompanied by progressive ipsilateral thoracolumbar pain and abdominal numbness. She previously underwent a thoracotomy for a T10 paraspinal fibroma, 6.5 years prior. On examination, the patient endorsed tenderness to palpation of the left-sided thoracolumbar mass but was otherwise neurologically intact.

Imaging

CT revealed an irregularly shaped soft-tissue mass (61.0 × 47.7 × 77.4 mm, hyperdensity 38.4 HU) immediately left to the spine at T9–T11 (Fig. 9.1f). CT with contrast demonstrated heterogeneous enhancement, and areas of hypodense necrosis were identified. Lytic invasion of the left posterolateral T10 and T11 vertebral bodies was identified, with extension into the pedicles (Fig. 9.1g). The left paraspinal muscles from T9 to L2 were noted to be wider than the contralateral side. MRI similarly revealed a large soft-tissue mass (112.7 × 104.3 × 62.6 mm) with irregular margins from T9 to T11 (Fig. 9.1a). The lesion was T1 hypo-intense, T2 hyper-intense, and DWI hyper-intense. Soft-tissue infiltration was noted through the left T10/T11 neural foramen, resulting in epidural spinal cord compression. At the levels of T9–L2, an irregularly shaped, multi-lobular soft-tissue mass was found in the left paraspinal muscles (Fig. 9.1b, c).

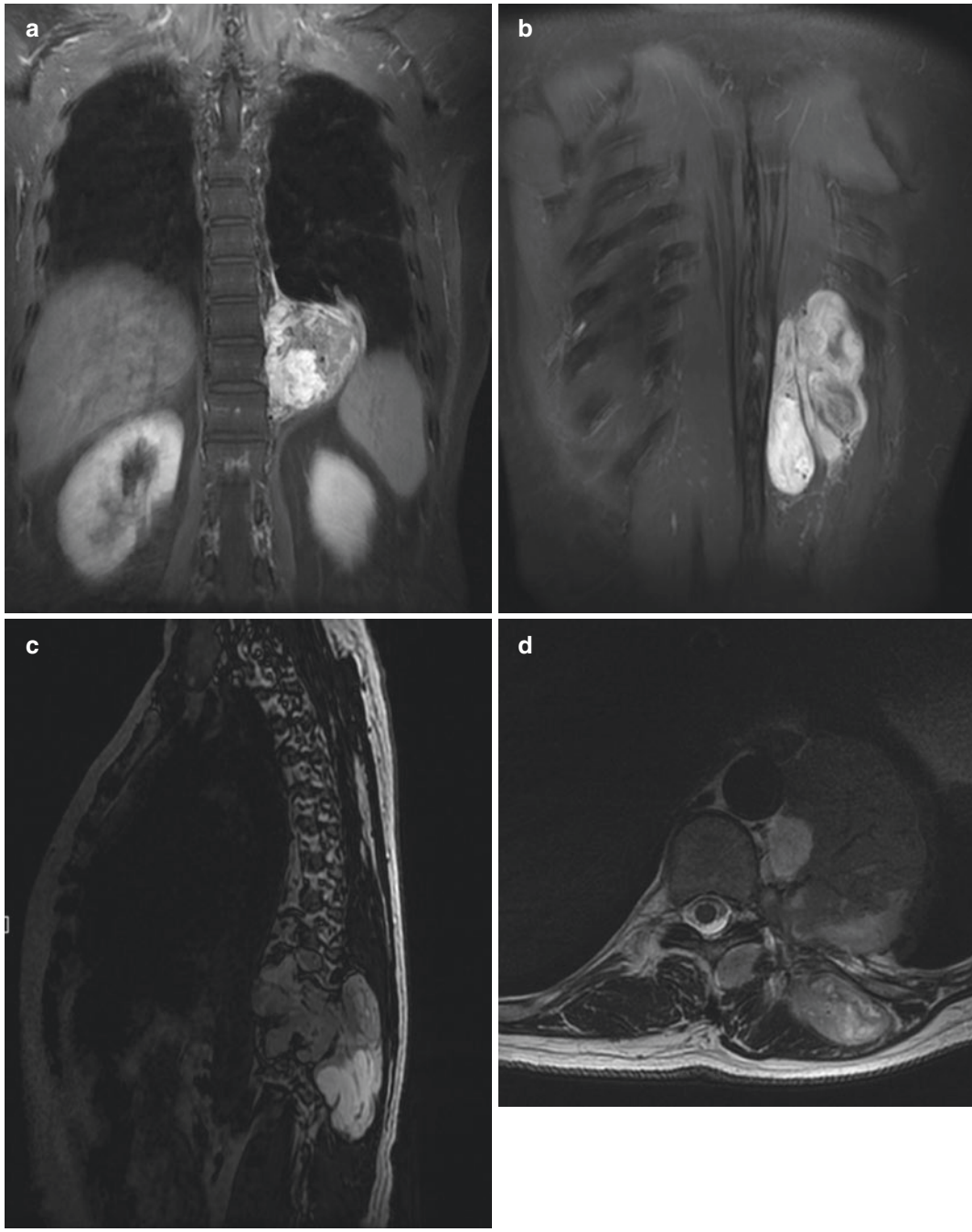

Fig. 9.1 Images of the patient on initial presentation, including magnetic resonance (**a**–**e**) computed tomography of the thoracic spine. (**a**) Image of magnetic resonance in the coronal plane shows the tumor on the left side of the vertebral body of T9 – T11. (**b**) Image of magnetic resonance in the coronal plane shows the tumor in the iliocostalis thoracis which reaches the level of L1 – L2. (**c**) Image of magnetic resonance in the sagittal plane shows the tumor in the iliocostalis thoracis, which reaches the level of L1 – L2. (**d**) Image of magnetic resonance in the axial plane of T9. (**e**) Image of magnetic resonance in the axial plane of T10 – T11. (**f**) Image of computed tomography in the axial plane of T9. (**g**) Image of computed tomography in the axial plane of T10 – T11. The black arrow shows the position of the diaphragm. (**h**) Image of computed tomography in the coronal plane shows the tumor on the left side of the vertebral body of T9 – T11. The white arrow shows the position of the diaphragm. (**i**) Image of computed tomography in the sagittal plane. The white arrow shows the position of the diaphragm, which reveals that the tumor is above the diaphragm

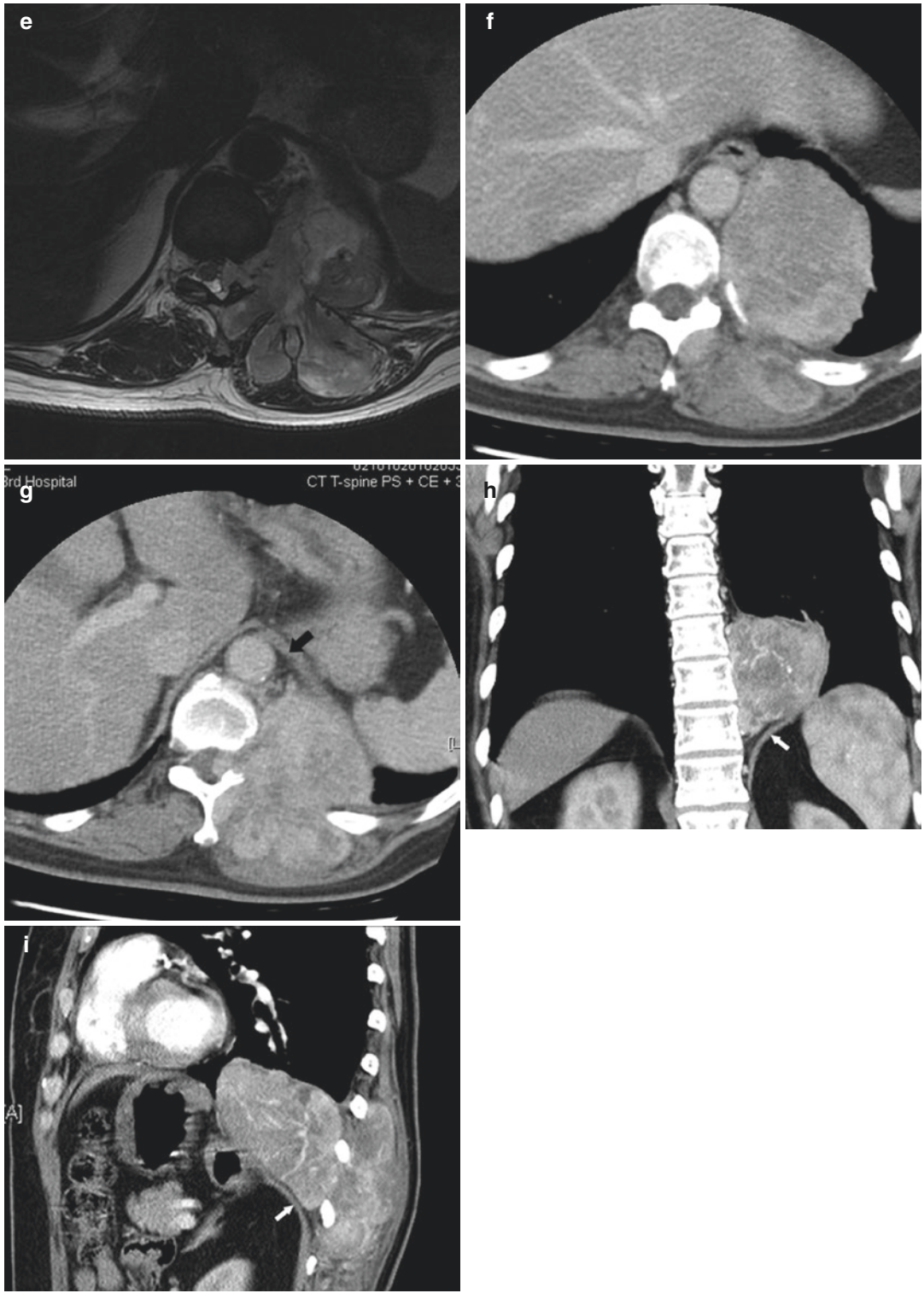

Fig. 9.1 (continued)

Pathologic Diagnosis

Pathology slides from the previous surgical resection were not available for review. A CT-guided biopsy was therefore performed, which revealed a spindle-cell mesenchymal tumor with profuse stromal vascularity, determined by the numerous branching vessels. There was no significant pleomorphism, and the extracellular matrix was collagenous. These characteristics suggested the diagnosis of a solitary fibroma. Even though the tumor cells were not highly mitotic (low Ki-67), large (>10 cm) extrapleural solitary fibromas are generally considered aggressive, and an intracapsular surgical resection with positive margins is associated with a sub-optimal prognosis. These tumors were called hemangiopericytomas because of their profuse stromal angiogenesis, and an intracapsular resection will likely lead to significant intraoperative blood loss. A plan for extracapsular en bloc resection was therefore determined as appropriate in order to reduce blood loss, prevent recurrence, and prolong tumor-free survival.

Tumor Staging and Surgical Planning

The tumor was Enneking S3 and WBB 1–6, A–D (Figs. 9.1d, e and 9.2a). In accordance with the WBB guidelines for resection of thoracolumbar

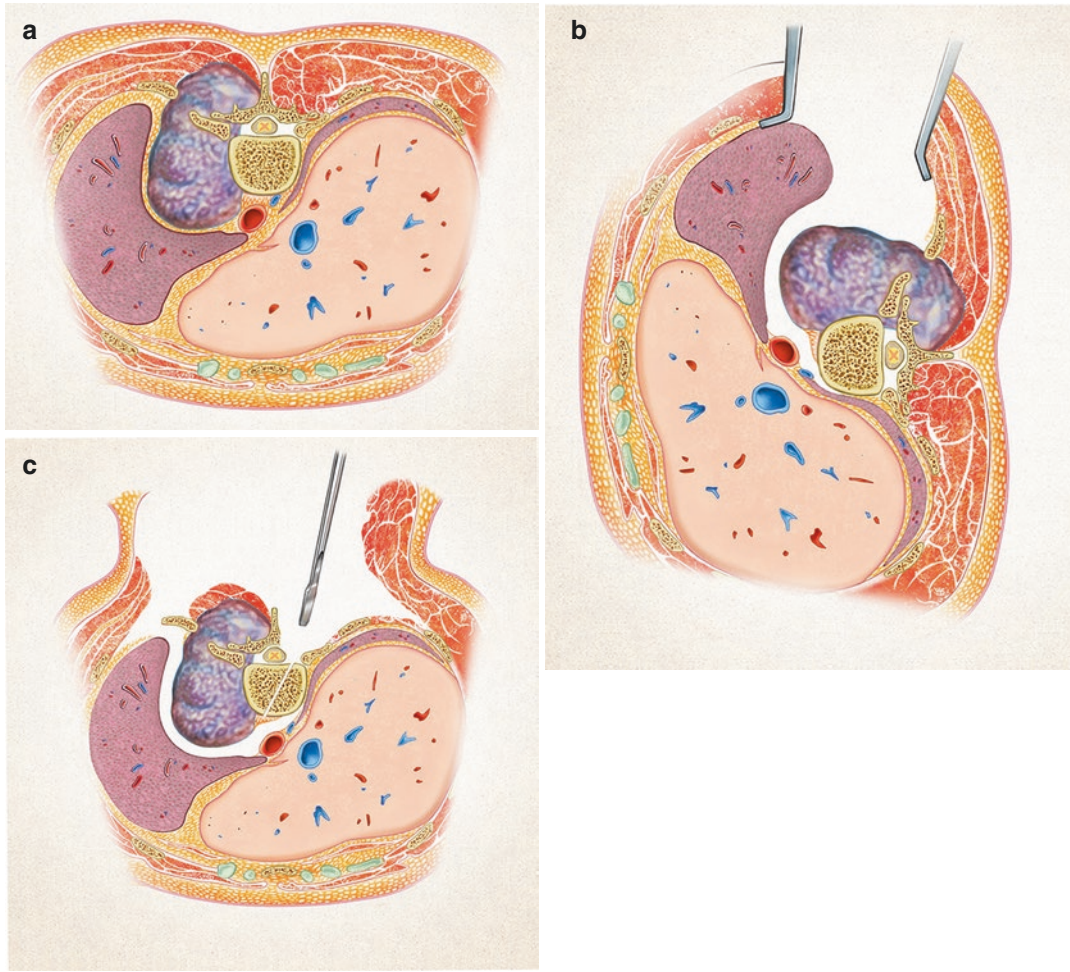

Fig. 9.2 Illustration of the tumor and stages of the surgery. (**a**) The illustration shows the tumor involving the wide areas of the lateral side of the vertebral body, appendix, and the intervertebral foramen. (**b**) Stage 1 operation involving left-sided thoracotomy and tumor released from the lung, aorta, diaphragm, and vertebral body. (**c**) Stage 2 operation involving the sagittal en bloc resection via posterior approach

tumors, a detailed surgical plan was adopted. In the first stage, an anterolateral approach was taken to separate the tumor from adjacent normal structures including the left lung, diaphragm, and aorta (Fig. 9.2b). In the second posterior stage, a plane was developed between the superficial and deep paraspinal muscles, advanced anterolaterally until the tumor was circumferentially released. The right posterior elements that were not involved by the tumor were removed in a piecemeal fashion to reveal the neural structures. The involved levels were separated from the normal spine by proximal and distal discectomies, and a sagittal osteotomy was performed diagonally from the right posterior to the left anterior in the involved vertebrae (Fig. 9.2c). The tumor mass was taken out en bloc from the posterior approach.

Preoperative Optimization

Feeding arteries to the tumor were selectively embolized by an interventional radiologist one day prior to the first stage. Angiography demonstrated a large tumor with proficient blood supply from the T9–T11 intercostal arteries, which were embolized using N-butyl cyanoacrylate (300–500 μm in size) and coils (Fig. 9.3).

Operative Technique

First stage: The patient was placed on right lateral decubitus and under general anesthesia with double-lumen endotracheal intubation. The T10 vertebra (where tumor diameter was the largest) was found to correspond to the level of the 8th rib on the mid-axillary line. A 15-cm incision through the skin, subcutaneous fascia, and the latissimus dorsi was made along the left 8th rib, centering on the mid-axillary line. The 8th rib was exposed and excised by about 12 cm. Following deflation of the left lung, the parietal pleura was opened to enter the thoracic cavity (Fig. 9.4). Electrocautery was used to dissect the adhesions between the tumor and the left lung. Manual palpation was utilized to identify the lower margin of the tumor, between the caudal aspect of the tumor and diaphragm. Because the aorta was dorsal to the tumor and not under direct visualization, blunt finger dissection helped separate the tumor

Fig. 9.3 Embolization of the segmental arteries of the left side

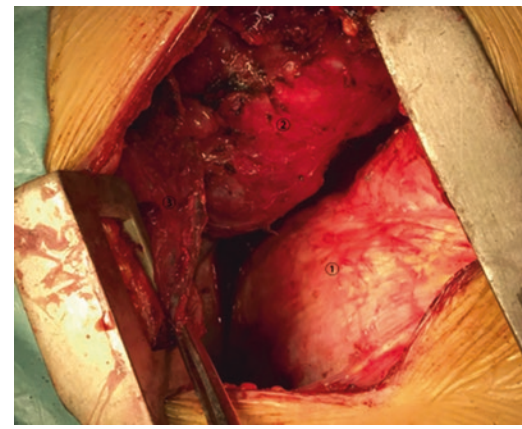

Fig. 9.4 Operative photograph of left-sided thoracotomy. ① diaphragm; ② tumor; and ③ lung

from the aorta and spine. Due to the preoperative embolization, only limited venous bleeding was encountered during the first-stage procedure. The parietal pleura and intercostal muscles were dissected, using electrocautery, with a 1-cm margin proximally and laterally. The 9th, 10th, and the 11th ribs were partially resected, with rib-cutting forceps. Proximally, the T9/T10 intervertebral disc was identified by fluoroscopy, and a lateral partial discectomy was performed. The left half of the anterior longitudinal ligament was also resected. The space formed between the aorta and the involved vertebrae was packed with large amounts of Gelfoam for both hemostasis and to prevent adhesions during the second stage. The wound was closed in a layered fashion, and a chest tube was placed.

Second stage: Seven days following the first surgery, the patient was placed prone on the table under general anesthesia with double-lumen endotracheal intubation. A mid-line incision was made from T7 to L2, followed by subperiosteal dissection. With fluoroscopic assistance, right-sided pedicles were placed from T7 to L1. The right-sided screws from T9 to T11 were removed temporarily to allow subsequent osteotomy. A left transverse incision down to the latissimus dorsi, perpendicular to the mid-line, was extended laterally into the previous incision. The thoracolumbar fascia was exposed by reflecting the latissimus dorsi and serratus muscles cranially. The rib cut ends from the first-stage procedure could be palpated. The thoracolumbar fascia was incised lateral to the longissimus thoracis, from T7 to L2. The uninvolved, more superficial longissimus thoracis was divided from the deeper iliocostalis thoracis. The tumor was palpable deep into the iliocostalis thoracis from T9 to T12. The iliocostalis thoracis was transected proximally and distally with 1-cm margins to the tumor. The left T7–T8 laminae were exposed, and two pedicles screws were inserted. The distal cut end of the iliocostalis thoracis was cranially reflected, with the tumor exposing the left facet joints of T11–L1. Pedicle screws were inserted at T12 and L1.

The cut ends of the 9th to 11th ribs from the first stage were palpated, and the lateral 3 cm of the cut ends was resected further to allow access to the left thoracic cavity. Once the left lung was deflated, blunt dissection was utilized to free the tumor anteriorly, releasing the loose connective tissues between the tumor and the adjacent lung, diaphragm, aorta, and spine. Gauze was placed temporarily between the tumor mass and adjacent structures. The intercostal muscles were transected along the upper edge of the 9th rib and the lower edge of the 11th rib down to the level of the facet joints of T8/T9 and T11/T12, respectively. The involved intercostal vessels and nerves were sacrificed. The tumor mass was now completely freed from adjacent organs, anteriorly, and uninvolved back muscles, posteriorly.

Subsequently, the spinous process, lower half laminae, inferior articular processes of T8, and superior articular processes of T9 were resected using an ultrasonic blade. The T11/T12 intervertebral level was similarly released. Right hemilaminectomies and facetectomies were performed from T9 to T11. The right T9–T11 nerve roots were ligated, and the dural sac was released from the posterior longitudinal ligament using a Penfield elevator. The proximal (T8/T9) and distal (T11/T12) intervertebral discs and posterior longitudinal ligament at the corresponding levels were resected. The proximal release was easier since part of the T8/T9 disc and the anterior longitudinal ligament was resected in the first stage. The T11/T12 disc was not accessible during the first stage, and the anterior longitudinal ligament at that level was resected from the posterior approach. In order to prevent injury to the aorta, an abdominal spatula was inserted along the cut ends of the ribs and placed between the aorta and the spine, before the anterior annulus fibrosus and longitudinal ligament were transected with an osteotome. The left half of T9–T11 vertebrae and their posterior elements were now ready to be removed en bloc with sagittal resection. According to CT-based preoperative planning, an osteotomy line from the medial wall of the pedicles to the left anterior part of the vertebral body with a 30° angle from the vertical axis of the patient body would allow sufficient distance from the tumor margin. An ultrasonic blade was used to perform osteotomies of the T9–T11 vertebral bodies, while the dura and aorta were protected

with a nerve elevator and an abdominal spatula, respectively. Partial discectomies of T9/T10 and T10/T11 were performed using a No. 15 blade scalpel and a pituitary rongeur. The entire tumor mass, including the left half of T9–T11 vertebrae, posterior elements, and proximal ends of the corresponding ribs, was mobilized.

A ball-tip probe was used to palpate the medial wall of the right pedicle screw tracts within the bodies of T9 and T11. Both were intact and the two screws were re-inserted. A precontoured connecting rod was placed and locked in on the right side. The tumor mass was gently pushed laterally until the left margin of the thecal sac and left T9–T11 nerve roots were visible. The nerve roots were ligated. After carefully releasing the adhesion with the dura, near the T10/T11 neural foramen, the tumor mass was taken out en bloc (Figs. 9.5 and 9.6).

The inferior endplate of T8 and the superior endplate of T12 were decorticated using a curette, and a 15-mm titanium cage with allografted bone was placed between T8 and T12. The left connecting rod was placed and locked in, with compression between T8 and T12. Two cross-links were used to brace the construct. In order to repair the defect in the left thoracic wall from the 10-cm resection on the 9th, 10th, and 11th ribs, two titanium rods mimicking the contour of ribs were connected to the left rod using dominos (Fig. 9.7). A hernia repair film was sutured to the rib rods and a chest tube was placed (Fig. 9.8). Our plastic surgeon colleagues used a retrograde latissimus dorsi musculocutaneous flap to repair the large paraspinal soft-tissue defect (Fig. 9.9). One Jackson-Pratt drain was placed underneath the surgical wound and one under the donor site.

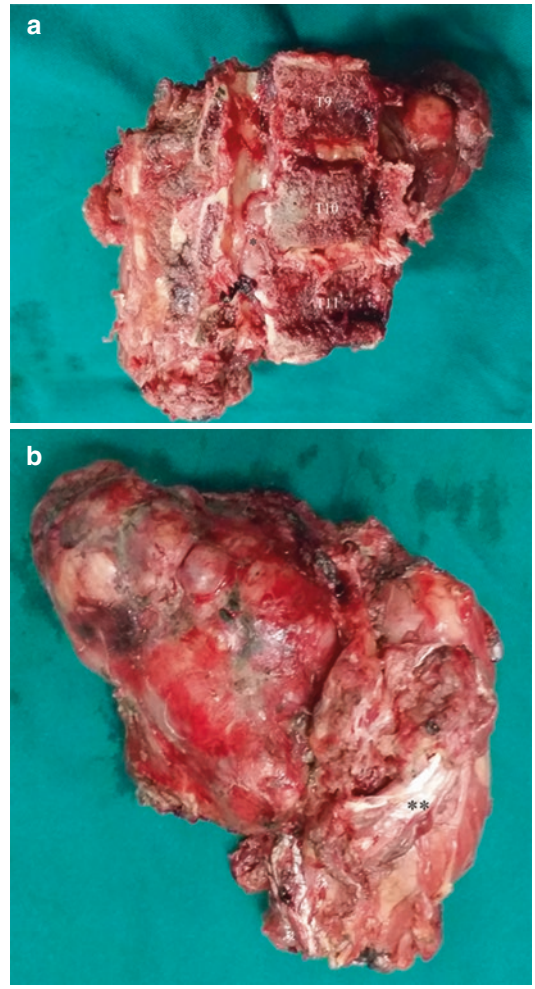

Fig. 9.5 Photographs of the removed specimen. (**a**) Sagittal view. The star (*) shows the tumor in T10 – T11 intervertebral foramen. (**b**) Lateral view. The double star (**) shows the iliocostalis thoracis embracing the tumor inside

Clinical Outcome

The patient was neurologically intact following the surgery. Within the first week, the chest tube and drains were discontinued and the patient began to ambulate. Postoperative X-ray and CT confirmed implant position (Fig. 9.10), and pathology review of the margins was negative for invasion of the tumor capsule. The patient was doing well 8 months postoperatively, with no signs of tumor recurrence or complication.

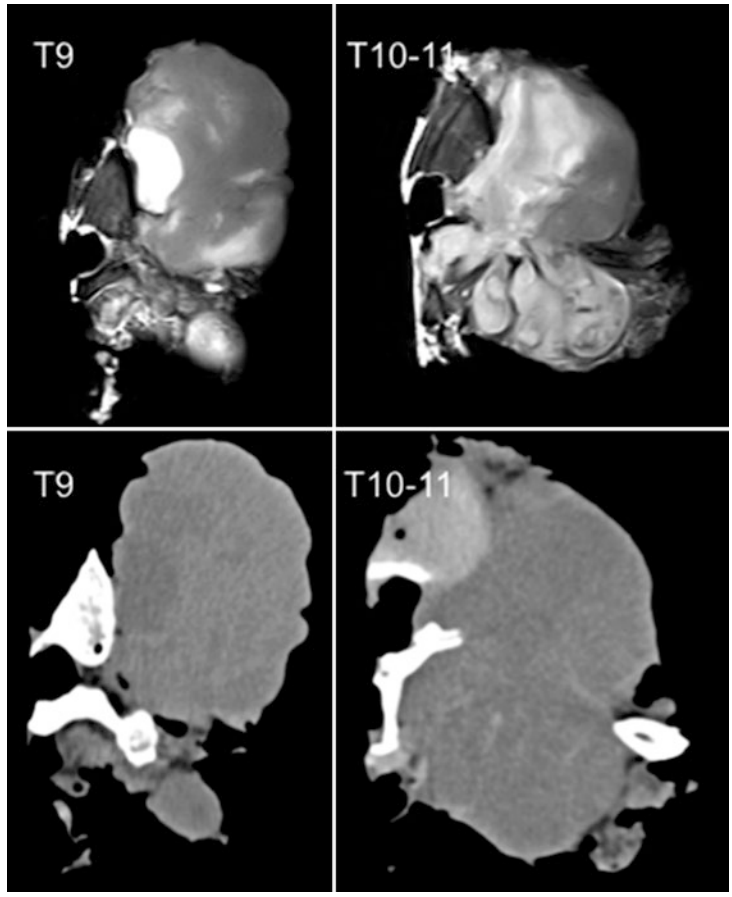

Fig. 9.6 Magnetic resonance of the removed specimen (the above two images) and computed tomography of the specimen (the below two images)

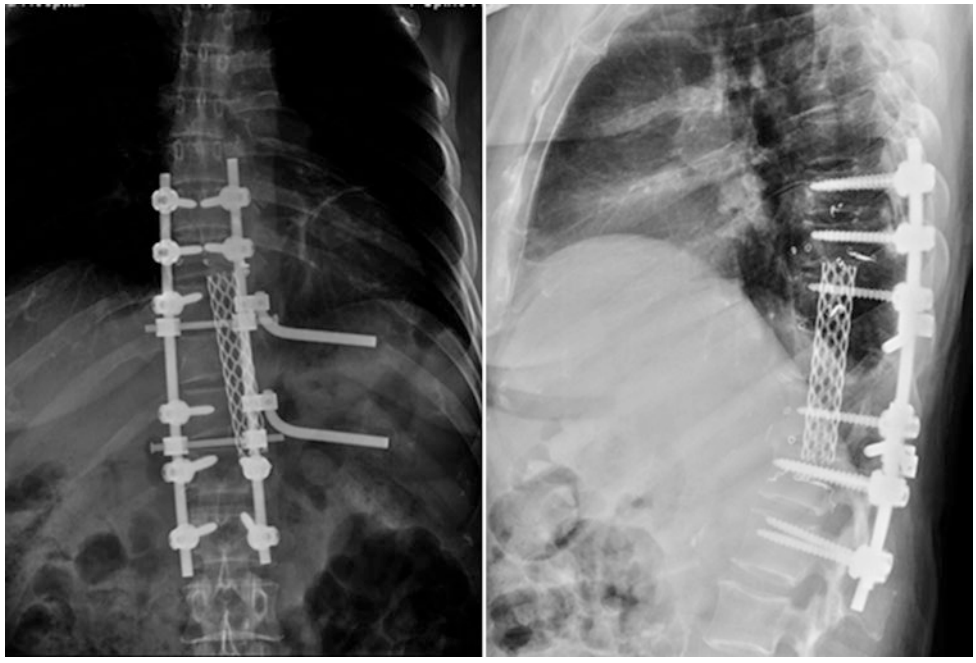

Fig. 9.7 The X-ray film of the final construct

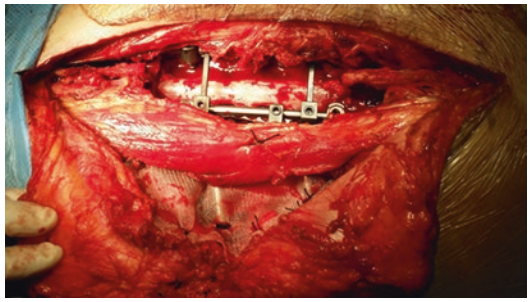

Fig. 9.8 Operative photograph of the surgery of the posterior approach

Fig. 9.9 Operative photograph of retrograde latissimus dorsi myocutaneous flap

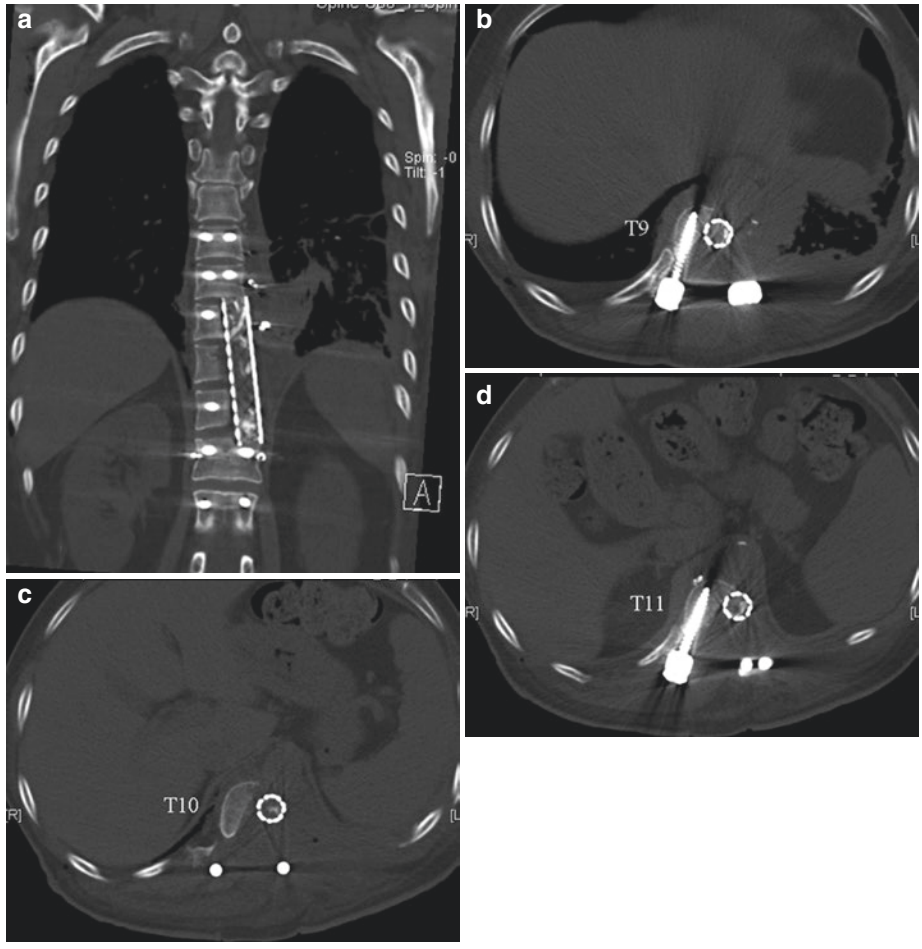

Fig. 9.10 The computed tomography of the final construct. (**a**) Coronal view. (**b**) Axial view of T9 level. (**c**) Axial view of T10 level. (**d**) Axial view of T11 level

Conclusion

Large thoracolumbar tumors involving at least three levels could be removed according to the WBB guidelines as staged procedures. An anterolateral trans-thoracic release could be performed first, followed by a posterior en bloc sagittal resection.

References

1. Vollmer DG, Banister WM. Thoracolumbar spinal anatomy. Neurosurg Clin N Am. 1997;8:443–53.
2. Willard FH, Vleeming A, Schuenke MD, Danneels L, Schleip R. The thoracolumbar fascia: anatomy, function and clinical considerations. J Anat. 2012;221:507–36.
3. Baaj AA, Papadimitriou K, Amin AG, Kretzer RM, Wolinsky JP, Gokaslan ZL. Surgical anatomy of the diaphragm in the anterolateral approach to the spine: a cadaveric study. J Spinal Disord Tech. 2014;27:220–3.
4. du Plessis M, Ramai D, Shah S, Holland JD, Tubbs RS, Loukas M. The clinical anatomy of the musculotendinous part of the diaphragm. Surg Radiol Anat. 2015;37(9):1013–20.
5. Lumsden AB, Colborn GL, Sreeram S, Skandalakis LJ. The surgical anatomy and technique of the thoracoabdominal incision. Surg Clin North Am. 1993;73:633–44.
6. Konig MA, Milz S, Bayley E, Boszczyk BM. The direct anterior approach to the thoracolumbar junction: an anatomical feasibility study. Eur Spine J. 2014;23:2265–71.
7. Dakwar E, Ahmadian A, Uribe JS. The anatomical relationship of the diaphragm to the thoracolumbar junction during the minimally invasive lateral extracoelomic (retropleural/retroperitoneal) approach. J Neurosurg Spine. 2012;16:359–64.
8. Fahim DK, Kim SD, Cho D, Lee S, Kim DH. Avoiding abdominal flank bulge after anterolateral approaches to the thoracolumbar spine: cadaveric study and electrophysiological investigation. J Neurosurg Spine. 2011;15:532–40.
9. Molina CA, Gokaslan ZL, Sciubba DM. Retroperitoneal approaches to the thoracolumbar spine. Neupsy key 2011. Available from: https://neupsykey.com/retroperitoneal-approaches-to-the-thoracolumbar-spine/
10. Fourney DR, Gokaslan ZL. Thoracolumbar spine: surgical treatment of metastatic disease. Curr Opin Orthop. 2003;14:144–52.
11. Walsh GL, Gokaslan ZL, McCutcheon IE, Mineo MT, Yasko AW, Swisher SG, et al. Anterior approaches to the thoracic spine in patients with cancer: indications and results. Ann Thorac Surg. 1997;64:1611–8.